

Ultrastructure and Large Subunit rDNA-Based Phylogeny of *Sphaerodinium cracoviense*, an Unusual Freshwater Dinoflagellate with a Novel Type of Eyespot

SANDRA C. CRAVEIRO,^{a,b} ØJVIND MOESTRUP,^c NIELS DAUGBJERG^c and ANTÓNIO J. CALADO^{a,b}

^a*GeoBioSciences, GeoTechnologies and GeoEngineering (GeoBioTec) Research Unit, University of Aveiro, P-3810-193 Aveiro, Portugal, and*
^b*Department of Biology, University of Aveiro, P-3810-193 Aveiro, Portugal, and*

^c*Section for Evolution and Ecology of Aquatic Organisms, Department of Biology, University of Copenhagen, Øster Farimagsgade 2D, DK-1353 Copenhagen K, Denmark*

ABSTRACT. *Sphaerodinium cracoviense* was collected near Cracow, Poland, and analysed by light microscopy, scanning electron microscopy, and serial-section transmission electron microscopy. Thecae showed a peridinioid type of plate arrangement with unusual numbers in the anterior intercalary and postcingular plate series: 4 and 6, respectively. The apical pore of *S. cracoviense* differed from the typical arrangement seen in many thecate forms and included a furrow with knob-like protuberances reminiscent of the apical area of some woloszynskioids. The flagellar apparatus included the three microtubular roots that extend to the left of the basal bodies and a striated root connective between the transverse striated root and the longitudinal microtubular root. Both the single-stranded root that associates with the right side of the longitudinal basal body in peridinioids and gonyaulacoids, and the layered connective typical of peridinioids were absent. The eyespot was formed by a layer of vesicle-contained crystal-like units underlain by layers of variably fused globules not bounded by membranes, and represents a novel type. The pusular system included a long canal with a dilated inner portion with radiating tubules. Bayesian and maximum likelihood analyses based on large subunit rDNA placed *Sphaerodinium* as a sister taxon to a group of woloszynskioids and relatively far from *Peridinium* and its allies.

Key Words. Bayesian analysis, dinoflagellate phylogeny, electron microscopy, flagellar apparatus, lamellar body, maximum likelihood, peridinioids, pusule, woloszynskioids.

THE genus *Sphaerodinium* was described by Wołoszyńska (1916), who described and named three new species and one variety, and noted one further species or variety that she did not name: *Sphaerodinium cracoviense*, *Sphaerodinium limneticum*, *Sphaerodinium polonicum* and *S. polonicum* var. *taticum*, and *Sphaerodinium* sp., all collected from several freshwater locations in Poland. The generic description was based on thecal features and included the description of all major thecal plates: in the epitheca, seven plates regularly arranged around a hexagonal plate (corresponding to plate 3' in Kofoidian notation) and seven precingular plates; in the hypotheca, six postcingular and two antapical plates. All species were described with an apical pore. The species were distinguished by Wołoszyńska (1916) on the basis of differences in general cell shape, plate ornamentation, and in the shape of the sulcus. The type species was not designated in this work and the genus was later typified by Loeblich and Loeblich (1966), who selected *S. polonicum* as lectotype. A further species was described by Wołoszyńska (1930) from tropical Sumatra, Indonesia, first incompletely, and later included by Schiller (1935) in his monograph as *Sphaerodinium javanicum* Wołoszyńska in Schiller (1935). Another species of *Sphaerodinium*, *Sphaerodinium fimbriatum* R.H. Thompson, showing the typical tabulation of the genus, was later described by Thompson (1951) from Kansas, USA. *Sphaerodinium* species have been infrequently reported from several fresh- and brackish-water localities scattered around the world: Ivory Coast (Couté and Iltis 1984), Burundi (Caljon 1987), Tasmania (Ling, Croome, and Tyler 1989), Belize (Carty and Wujek 2003), Austria (Tolotti and Thies 2002), and Hungary (Grigorszky et al. 2003).

Recent works combining external morphology, ultrastructure, and DNA-based phylogenies of peridinioids and woloszynskioids have led to changes in our understanding of phylogenetic relationships among species, with consequent taxonomic rearrangements (e.g. Calado et al. 2009; Craveiro et al. 2009a; Hansen, Daugbjerg, and Henriksen 2007; Lindberg, Moestrup, and Daugbjerg 2005). However, a complete understanding of the phylogenetic relationships within and between the peridinioids and

woloszynskioids has not yet been achieved. In this regard, *Sphaerodinium* is unusual in having a larger number of intercalary plates than is common in peridinioids, and in having six (rather than the usual five) postcingular plates. The relatively high number of thecal plates seems to place *Sphaerodinium* in an intermediate position between the peridinioids and the more thinly thecate woloszynskioids.

Therefore, the present article describes the general fine-structural organization and the flagellar apparatus of *S. cracoviense* as well as a novel type of eyespot. Thecal morphology is described as seen by scanning electron microscopy (SEM). Additionally, *Sphaerodinium* was included in a phylogeny reconstruction with Bayesian inference and maximum likelihood (ML) methods, prepared on the basis of partial large subunit (LSU) rDNA sequences. Preliminary results of this work were presented at IPC9 (Craveiro et al. 2009b).

MATERIALS AND METHODS

Biological material. *Sphaerodinium cracoviense* was found in high numbers in the plankton collected from two fishponds in Pieskowa Skala (Ojców National Park), north of Cracow, Poland (50°14'37"N, 19°46'45"E), in August 2007. All the observations and preparations were made with the cells from those samples or from a culture started with cells isolated to SC medium, a soil-water medium (Christensen 1962), and maintained at 15 °C with 16:8 light:dark photoperiod.

Light microscopy (LM). Cells from field samples and from the culture were observed and photographed in a Zeiss Axioskop light microscope with a Zeiss AxioCam HRC digital camera (Carl Zeiss, Oberkochen, Germany).

SEM. About 1.6 ml of the field material were fixed with a fixative mixture of 1:3 mixture of saturated HgCl₂ and 2% (w/v) osmium tetroxide in a proportion of 2:1, respectively, to the sample for 30 min. Another portion of field sample was fixed with Lugol's solution overnight. Cells from both fixations were retained on Isopore polycarbonate filters with 8-µm pore size (Millipore Corp., Billerica, MA), washed with distilled water, and dehydrated through a graded ethanol series. The cells were then critical-point-dried and the filters glued onto stubs using double-sided adhesive tape. After being sputter-coated with

Corresponding Author: A.J. Calado, Department of Biology, University of Aveiro, P-3810-193 Aveiro, Portugal—Telephone number: +351 2343 70785; FAX number: +351 2343 72587; e-mail: acalado@ua.pt

platinum-palladium for 90 s, the stubs were observed in a JEOL JSM-6335F (JEOL Ltd., Tokyo, Japan) SEM.

Transmission electron microscopy (TEM). Two fixation protocols were followed, both using swimming cells individually picked up from live field samples: (1) cells were transferred to 2% (v/v) glutaraldehyde in 0.1 M phosphate buffer, pH 7.2, and fixed for 1 h at 4 °C; and (2) cells were transferred to a mixture of 1% (v/v) glutaraldehyde and 0.5% (w/v) osmium tetroxide (final concentrations) in 0.1 M phosphate buffer, pH 7.2, and fixed for 1 h at 4 °C. Cells from both fixations were then rinsed in buffer, included in 1.5% agar blocks and postfixed in 0.5% (w/v) osmium tetroxide at 4 °C overnight. After being rinsed with 0.1 M phosphate buffer and distilled water, the agar-embedded cells were dehydrated through a graded ethanol series and propylene oxide and embedded in Spurr's resin. The blocks were sectioned with a diamond knife in an EM UC6 ultramicrotome (Leica Microsystems, Wetzlar, Germany). Ribbons of serial sections (70 nm thick) were picked up with slot grids and placed on Formvar film. The sections were stained with uranyl acetate and lead citrate. In total, serial sections of five cells were observed in a JEOL JEM 1010 TEM (JEOL Ltd.).

Single-cell polymerase chain reaction (PCR). One to three cells of *S. cracoviense* were isolated from starting cultures with low cell numbers, washed twice in double-distilled water, and transferred to 0.2-ml PCR tubes containing a 8- μ l droplet of double-distilled water. Before PCR amplification of nuclear-encoded LSU rDNA, tubes containing *Sphaerodinium* cells were heated for 10 min at 94 °C. The PCR cocktail was then added and the temperature profile included denaturing at 94 °C for 3 min, followed by 35 cycles of denaturing at 94 °C for 1 min, annealing at 55 °C for 1 min, and extension at 72 °C for 3 min. The PCR temperature profile ended with an extension step of 10 min (see Hansen, Daugbjerg, and Henriksen 2000 for details on chemicals and concentrations used). Amplification primers used were D1F and DinoND (for primer sequences see Hansen and Daugbjerg 2004; Hansen et al. 2000). Semi-nested PCR was formed using the primer combination D1F-D3B and D3A-ND1483 and the same temperature profile as outlined above but with only 18 cycles. Polymerase chain reaction reactions were visualized in an agarose gel containing ethidium bromide. Lanes containing PCR fragments of correct length compared with a molecular marker (viz. PhiX 174 HAE III) were purified with a NucleoFast 96 PCR Kit, following the recommendations of the manufacturer (Macherey-Nagel GmbH & Co. KG, Düren, Germany). Purified PCR products were aliquoted to reach a final concentration of 500 ng. Before being sent to the sequencing service provided by Macrogen (Seoul, Korea) they were air-dried. The sequencing primers were D1R, D2C, D3A, D3B, and 28-1483R (for primer sequences see Daugbjerg et al. 2000; Hansen et al. 2000).

Alignment and phylogenetic analyses. To infer the phylogeny of *S. cracoviense* we added its LSU rDNA sequence to an alignment comprising a total of 58 dinoflagellate species covering a diverse assemblage of thecate and naked taxa. Ciliates (four species), apicomplexans (five species), and a single perkinsid comprised the outgroup. In total, 1,157 base pairs (including introduced gaps) covering domains D1 and D3–D6 (sensu Lenaers et al. 1989) were analysed using Bayesian inference and ML. Bayesian inference used MrBayes (ver. 3.1.2; Ronquist and Huelsenbeck 2003) with 2×10^6 Markov Chain Monte Carlo generations with four parallel chains (one cold and three heated). A tree was sampled every 50th generation and by plotting the log likelihood values as a function of generations the InL values converged after 20,050 generations. Using this as the burn-in provided 39,600 trees. All of these were imported into PAUP* (vers. 4b.10; Swofford 2003) to produce a 50% majority rule consensus tree. Branch support values in terms of posterior probabili-

ties were also obtained from the 39,600 trees. Bayesian analysis was performed on the freely available Bioportal at <http://www.biportal.uio.no>. For ML analyses we used PhyML (ver. 3; Guindon and Gascuel 2003) with settings according to the results from running our data matrix through Modeltest (ver. 3.7; Posada and Crandall 1998); the best-fit model was TrN+I+G, selected by hierarchical likelihood ratio tests. Parameters for proportion of invariable sites ($I = 0.2178$) and among site rate heterogeneity ($\alpha = 0.6465$) were used in PhyML. Support for the topology in ML was obtained by bootstrap analyses with 500 replications. The consensus programme from Phylip (ver. 3.68; Felsenstein 2008) was used to draw a 50% majority rule consensus tree.

RESULTS

Observations in LM. Cells of *S. cracoviense* were spherical to oval and slightly compressed dorsoventrally (Fig. 1, 2). Length of cells ranged from 24 to 31 μ m, width from 22 to 28 μ m, and thickness from 24 to 25 μ m. The cell surface was underlain by numerous yellowish-brown chloroplast lobes (thin arrows, Fig. 2). In the sulcal area there was a conspicuous, red, curved eyespot (Fig. 1, 2). The theca was generally thin and the plate arrangement was only discernible in empty thecae. Boundaries between cingular plates were difficult to observe and seemed somewhat variable, especially in the distal, right-hand side. The limits of the last two cingular plates are shown for one cell (thin arrows, Fig. 3).

Stereo-microscope observations revealed a marked positive phototactism, as virtually all cells in the middle of a watch-glass moved along parallel lines towards the light source.

Morphology and thecal structure (SEM). Cells were usually spherical with the nearly equatorial cingulum delimiting an epi- and hypotheca of almost equal size (Fig. 4–6). The cingulum descended nearly its own width at the right-ventral side of the cell (Fig. 4, 5). In ventral view the epitheca was slightly twisted to the left with precingular plate 7 partly aligned with the sulcus (Fig. 4, 5). Epithecatal tabulation was nearly symmetric with the four apical plates surrounding the apical complex (arrow, Fig. 7). Four dorsally located, similar-sized intercalary plates (1a–4a), together with apical plates 1, 2, and 4, formed a ring around apical plate 3 (Fig. 6, 7). Eight plates contacted the upper edge of the cingulum; seven of these are here labelled precingular. The remaining plate was directly aligned with the elongated plate 1' and is here labelled Z (Fig. 4, 5). The hypotheca had six postcingular and two antapical plates (Fig. 8). The thecae opened along the anterior border of the cingulum, often resulting in empty thecae with the epi- and hypotheca connected only by the sulcal plates (Fig. 9). Four plates were labelled as sulcal (Fig. 10, 11); this excludes a small plate between the left part of the sulcus and the proximal part of the cingulum, here considered cingular plate 1, and the plate labelled Z (see "Discussion"). The margins of postcingular plates 1 and 6, bordering the sulcus, were raised (Fig. 4, 8, arrows). The posterior sulcal plate (ps) was V-shaped in the posterior side and ended between the two antapical plates (Fig. 4, 11). The anterior sulcal plate (as) was small and round (Fig. 4, 10, 11). The right sulcal plate (rs) was directly aligned with the distal end of the cingulum, whereas the left sulcal (ls) extended from cingulum level to below the middle of the sulcus (Fig. 4, 10, 11).

The number of cingular plates was difficult to ascertain because the sutures were difficult to see even in SEM. Considering the very short plate in the beginning of the cingulum (c1, Fig. 10, 12) as a cingular plate, a maximum of eight cingular plates was counted in several cells. Although in some cells a smaller number of cingular plates was visible, all cells displayed a large plate covering the dorsal side of the cingulum, roughly corresponding to the length of postcingular plates 3 and 4.

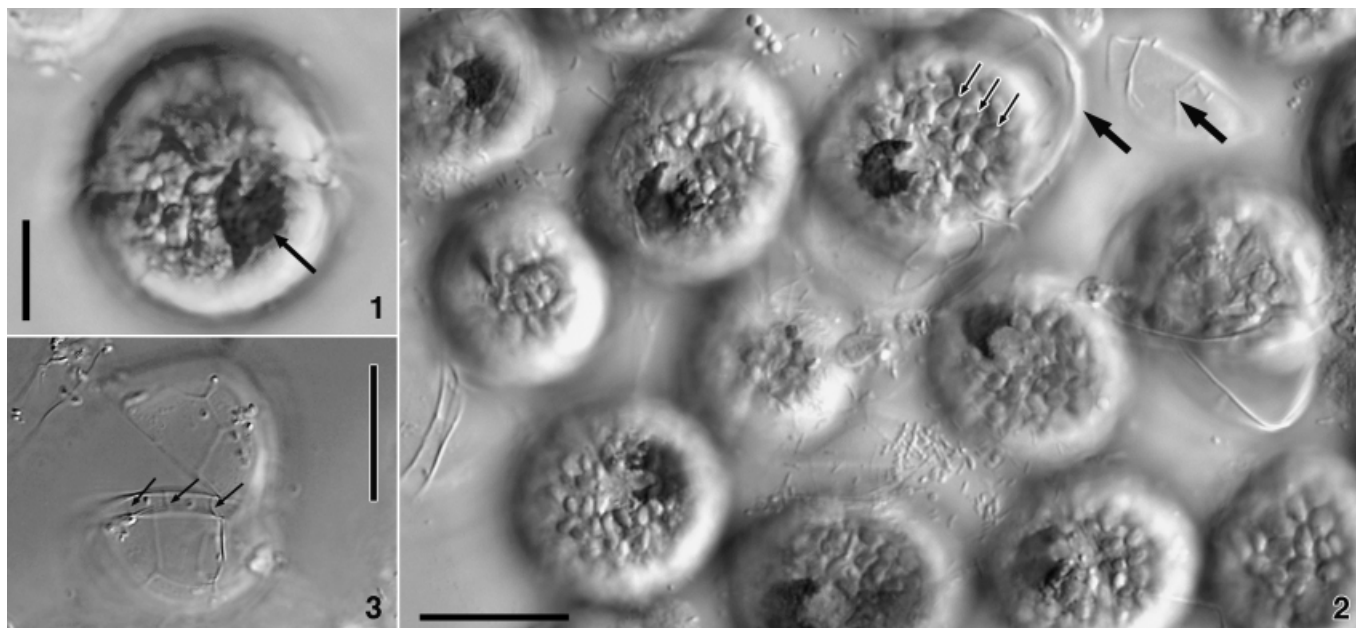


Fig. 1–3. *Sphaerodinium cracoviense*, light microscopy (LM). Live cells and thecae from field sample. **1.** Ventral view of a cell showing the conspicuous eyespot in the sulcal area. Scale bar = 10 μm . **2.** Several cells showing the eyespot and surface chloroplast lobes (thin arrows). Note detached thecae with visible plate sutures (thick arrows). Scale bar = 20 μm . **3.** Ecdysed theca opened along the upper edge of the cingulum with sulcal plates connecting epi- and hypotheca. Three cingular sutures on the right-hand side of the cingulum are visible (arrows). Scale bar = 20 μm .

On the basis of observations on cells stripped of the outer membranes, the apical complex was apparently composed of three plates: a small, central, elongated plate (labelled 1, Fig. 13, 14), 1 μm long and 0.3 μm wide, with a furrow along the middle; a larger plate that almost completely surrounded the first one (marked 2, Fig. 13, 14), and a medium-sized rectangular plate contacting the ventral edge of the other two plates (marked 3, Fig. 13, 14). In cells fixed to preserve the outer membranes the limits between these plates was more difficult to see; a row of knob-like protuberances, about 60 nm in diameter, is visible along the length of plate 1 (thin arrows, Fig. 13).

Thecal ornamentation consisted mainly of scattered trichocyst pores and knob-like protuberances that were visible only in thecae that retained the outer membranes (Fig. 4–8, 13). In thecae without outer membranes the plates were somewhat rugose due to tiny and irregular granules covering much of the surface (Fig. 10, 12, 14). Sutures between plates were mostly thin (Fig. 4–8) although somewhat wider sutures not showing any cross-striation were observed (Fig. 10).

General ultrastructure. General ultrastructural features of *Sphaerodinium* were typical of dinoflagellates (Fig. 15). The ellipsoid nucleus was located in the dorsal side of the cell at cingulum level (Fig. 15). Figure 16 shows simple nuclear pores in the nuclear envelope. Chloroplast profiles were mainly located at the periphery, connected to inward radiating lobes that did not invade the cytoplasm in the centre of the cell; there were no distinct pyrenoids but thylakoid-free areas were found in some chloroplast lobes (Fig. 15). Relatively large ellipsoid vesicles with diffuse granular contents were common between the chloroplast lobes at the periphery of the cell (Fig. 15). Trichocysts were abundant and bacteria were found in the cytoplasm of all cells (Fig. 15, 42). A few relatively small accumulation bodies were seen, both in the epi- and in the hypocone (ab, Fig. 15). Starch grains were small and more numerous near the antapex (Fig. 15). Opaque microbodies, apparently associated with translucent vesicles, formed a well-developed network in the central cytoplasm,

in the ventral region, and around the nucleus (thick arrows, Fig. 15, 42).

Apical complex. The three plates of the apical complex shown in SEM were identifiable in serial longitudinal sections through the cell apex (Fig. 17–20). The cytoplasm projected through the middle of plate 1 (Fig. 17–19), perhaps as a sequence of knob-like protuberances (Fig. 18, 19). In the apical region the cytoplasm showed vesicles with tubular extensions adjacent to amphiesmal vesicles (arrowheads, Fig. 18, 19).

Flagellar apparatus. A schematic reconstruction of the flagellar apparatus and related structures, as viewed from the left side of the cell, is presented in Fig. 21. The same point of view is shown in Fig. 22–29. Particular features of the flagellar apparatus are shown as viewed from the left-anterior side of the cell in Fig. 30–35. As estimated from serial sections, the angle between the basal bodies was about 90°, except in one cell, for which the angle of insertion of the basal bodies was nearly 140°.

Each flagellum emerged from the cytoplasm into a flagellar canal, which opened to the outside of the cell through a pore encircled by conspicuous fibrous material that was striated in at least some orientations, called transverse striated (TSC) and longitudinal striated collars (LSC), respectively. The TSC had a striated extension that covered partially the proximal part of a tube extending from the transverse flagellar canal into the cell (Fig. 22–24, 31–33, pusule tube). Both collars were connected by a surface opaque structure here interpreted as a ventral ridge (Fig. 21, double arrow in Fig. 37, 45). The ventral ridge was about 140 \times 40 nm in cross-section, and extended about 1 μm longitudinally along an area where the amphiesmal vesicles did not meet, between the posterior side of the TSC and the ventral surface of the LSC (Fig. 21, 37, 45). There were no visible microtubules associated with it.

Two single-stranded microtubular roots were associated with the transverse basal body (TB) and a single multistranded one with the longitudinal basal body (LB). The longitudinal microtubular root (LMR, r1 in Moestrup 2000), a multistranded

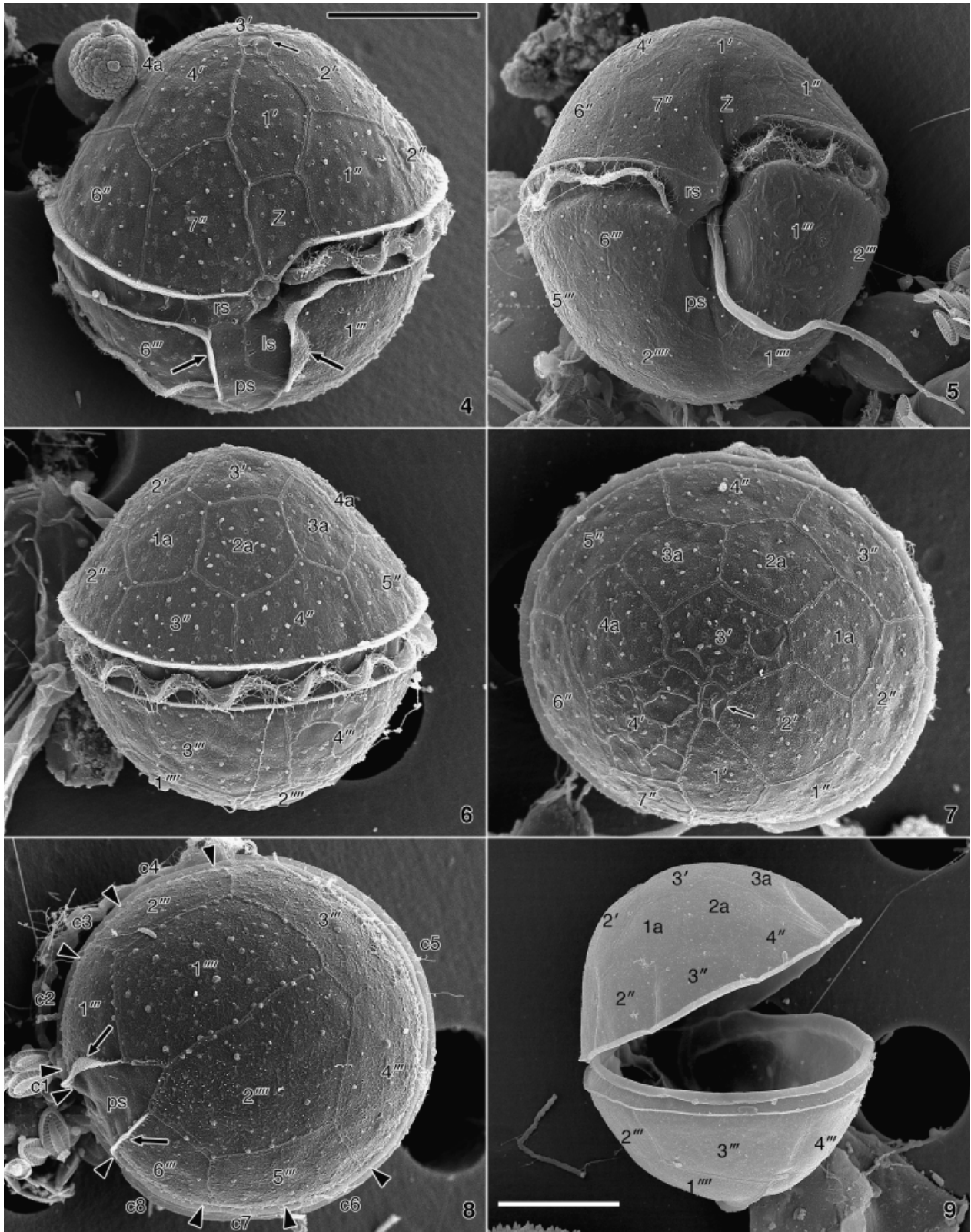


Fig. 4–9. *Sphaerodinium cracoviense*, scanning electron microscopy (SEM). rs, ls, ps, respectively, right, left, and posterior sulcal plates. The scale bar in Fig. 4 applies to all figures except Fig. 9. Scale bars = 10 μ m. 4. Ventral-anterior view. The apical complex is visible (arrow). The ventral plate contacting the upper edge of the cingulum and plate 1' is labelled Z. Thick arrows, raised edges of plates 1''' and 6''' bordering the sulcus. 5. Ventral view of a cell with a thin theca, showing a more extensive longitudinal depression on the ventral side. 6. Dorsal view showing the four anterior intercalary plates. 7. Apical view showing the six postcingular plates and the posterior end of the sulcus indenting the suture between the antapical plates. Arrowheads indicate the approximate position of the maximum number of cingular sutures detected. Thick arrows, raised edges of plates 1''' and 6''' bordering the sulcus. 9. Theca opening along the upper edge of the cingulum with epi- and hypotheca still connected in the sulcal area.

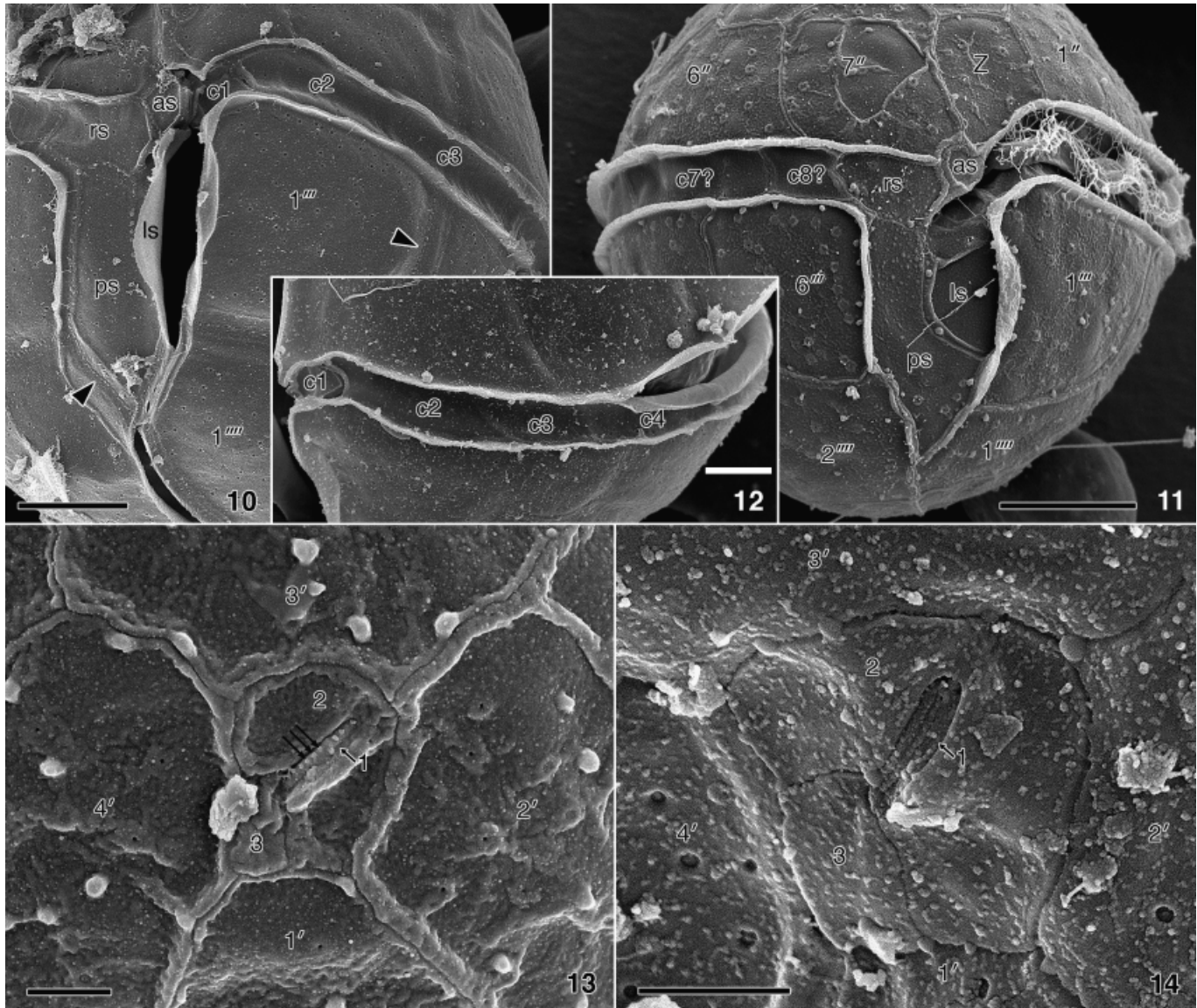


Fig. 10–14. *Sphaerodinium cracoviense*, scanning electron microscopy (SEM). as, rs, ls, ps, respectively, anterior, right, left, and posterior sulcal plates. **10.** Sulcal region with four visible sulcal plates. The very small plate on the top left corner of the sulcus is labelled cingular plate 1 (c1). Smooth sutures between plates are visible with thin contact lines bearing rows of tiny granules (arrowheads). Scale bar = 5 μ m. **11.** Ventral view of an intact sulcal area. Scale bar = 5 μ m. **12.** Left side of the cingulum showing the first four cingular plates (not detectable in all cells). Scale bar = 3 μ m. **13, 14.** Apical complex in a cell prepared to preserve outer membranes (Fig. 13) and in one stripped of outer membranes (Fig. 14). The three apical complex platelets are labelled 1–3. Note a row of small knobs in plate 1 in Fig. 13. Scale bars = 1 μ m.

microtubular root, associated with the left, anterior end of the LB, passed close to the dorsal side of the LSC and extended along the sulcal area towards the antapex (Fig. 21–29). The number of microtubules of the LMR increased from about eight at the proximal end to an estimated maximum of 36 (Fig. 21, 36). The transverse microtubular root (TMR, r3 in Moestrup 2000) started next to the anterior-proximal end of the TB, ran parallel to it for about 400 nm and then curved towards the apex, passing adjacent to a row of collared pits on the TFC (Fig. 25–27); the TMR then curved towards the dorsal side, running parallel to the pusule canal (Fig. 21, 33, 34). The TMR nucleated six or seven rows of four to eight microtubules each, collectively designated the transverse microtubular root extension (TMRE), which ran in a dorsal direction (Fig. 21, 24, 25, 33–35). The transverse striated root and

its associated microtubule (TSR and TSRM, r4 in Moestrup 2000) extended from the posterior side of the TB along the dorsal side of the TSC, close to the ventral cell surface, to the left side of the cell for nearly 1.6 μ m (Fig. 21, 23–28).

The striated root connective (SRC) connected the dorsal surface of the LMR to the posterior side of the TSR, close to the point where it attached to the TB (Fig. 21, 25–27). The proximal part of the LMR, next to the connection to the SRC, was covered by opaque material with a layered appearance (double arrow, Fig. 26).

A ventral fibre (VF, so called in the sense of Hansen et al. 2007) was present contacting the right-anterior side of the LB and progressing in a ventral-posterior direction, ending close to the ventral-right side of the TFC (Fig. 21, 28, 29, 37, 38). Two triplets on

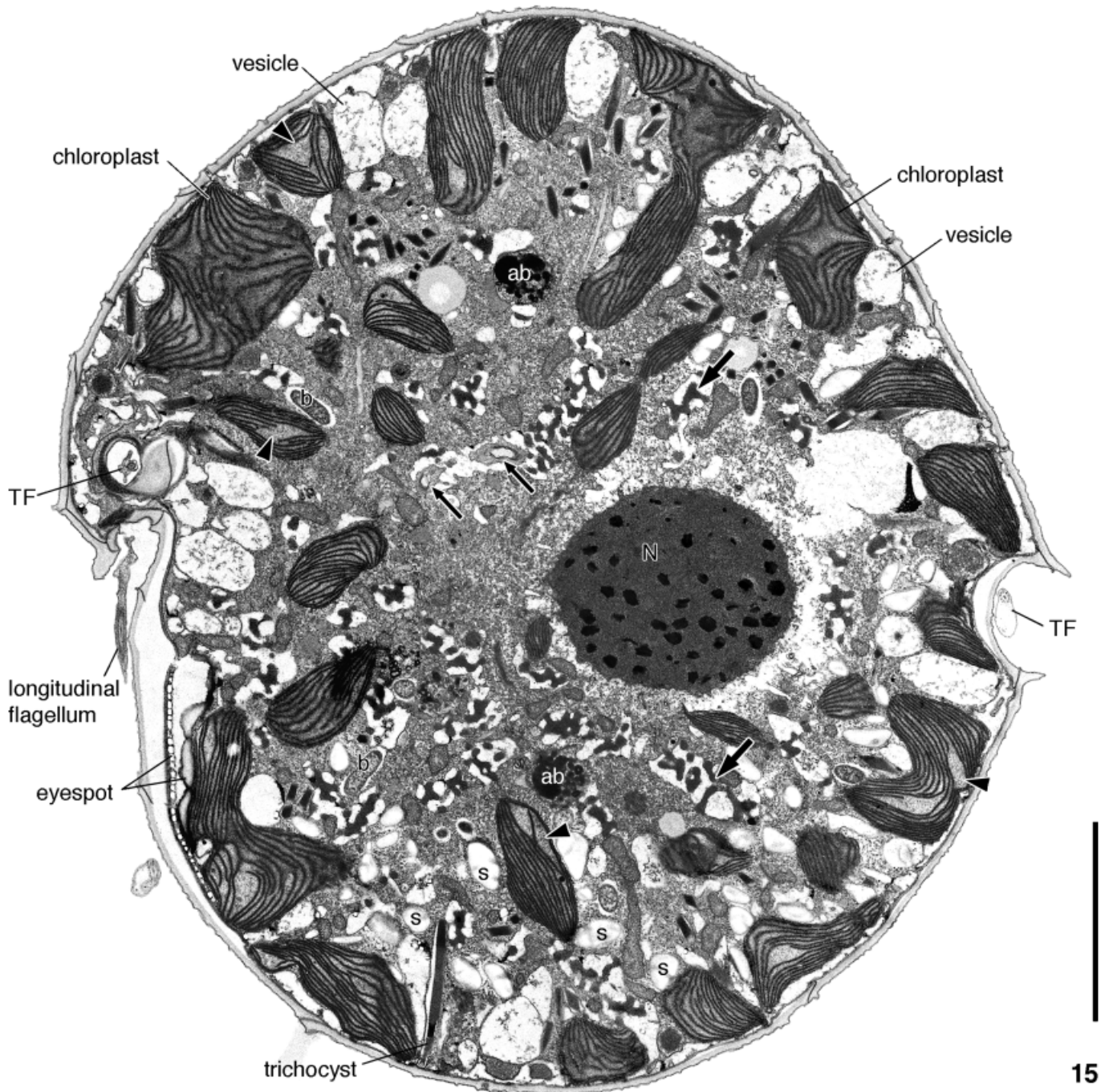


Fig. 15. *Sphaerodinium cracoviense*, transmission electron microscopy (TEM). General ultrastructure. Longitudinal section viewed from the left, showing both longitudinal and transverse flagella (TF), the eyespot beneath the sulcus, chloroplast profiles, the nucleus (N), bacteria (b) in the cytoplasm, starch grains (s) mainly in the hypocone, accumulation bodies (ab), and trichocysts. Thin arrows point to two segments of the pusule canal. Arrowheads mark thylakoid-free areas of chloroplasts. Note the number of electron-dense microbodies (thick arrows) distributed mainly in the central part. Scale bar = 5 μ m.

the ventral-right side of the LB were linked by thin fibres to the VF and two dorsal-left triplets displayed fibrous associations with the ventral side of the LMR (Fig. 21, 37–39); all these fibrous connections were 200–380 nm long.

Microtubular strand (ms). A wavy strand of about 15 microtubules, the ms was found along the anterior surface of the transverse collar extension that covered the pusule canal, curving

around the ventral side of the TSC and ending close to its posterior surface (Fig. 21, 22–25, 30–34). Although microtubules of the TMRE were in some places <200 nm from the microtubules of the ms, no visible connection was found between this strand and any other structure (Fig. 21, 25, 30–34).

Lamellar body. A structure formed by groups of parallel, tubular membranous components, each about 55 nm wide, was

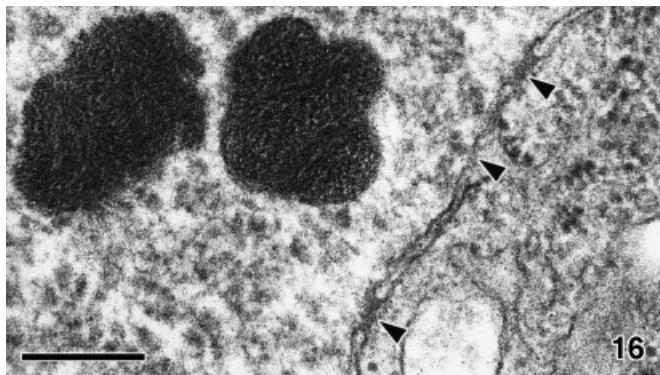


Fig. 16. *Sphaerodinium cracoviense*, transmission electron microscopy (TEM). Detail of the nuclear envelope showing nuclear pores (arrowheads). Scale bar = 200 nm.

found in the flagellar base area of all cells examined. Transverse sections through this structure showed a honeycomb pattern with an opaque body in the centre of each tubule (Fig. 21, 37, 38, 40). A less striking, lamellate appearance was found in longitudinal sections of the cell, which were also approximately longitudinal sections of the tubular elements of the lamellar body (Fig. 41, 42). As determined in serial sections, between four and seven independent fragments of lamellar body were found in the cells examined (Fig. 42, 45).

Eyespot. The eyespot occupied a large area, up to 10 μm long, underneath the sulcus (Fig. 19, 42–44). It was made of two types of components, none of them included in a chloroplast lobe. Ventralmost was a single layer of crystal or brick-like elements, apparently tightly packed inside a flat vesicle located immediately under the LMR or subthecal microtubules (Fig. 44). The brick-like elements were nearly square, some 130–180 nm wide and 90 nm thick. One to three irregular layers of more or less extensively fused oil globules underlay the brick layer (Fig. 42–44). As measured in transverse sections, individual oil layers, when more than one was present, were about 150 nm thick, with their middle lines approximately 240 nm apart. When only one layer was found, perhaps the result of fusion of several individual layers, thickness was around 450 nm. One chloroplast lobe was adjacent to the innermost oil layer in most of the eyespot area (Fig. 15, 42, 44).

Pusular system. There were two different sets of pusular structures, each one associated with one of the flagellar canals. A tube, here called pusule canal, with a lumen diameter of 250–390 nm opened at the anterior-dorsal side of the TFC (Fig. 21–24, 32, 33). The pusule canal was lined by a single membrane and covered by a layer of microfibrillar material (Fig. 48). It extended for nearly 4 μm from the ventral area to the dorsal-right side of the cell (Fig. 19, 22, 45), then curved to the left for 3 μm , and ended in a ventral location relative to the nucleus. In its distal end, the pusule canal enlarged into a collecting chamber, also lined by a single membrane, ca 800 nm long and 500 nm wide. Some 40 pusular tubules, each with a diameter of about 100 nm, radiated from the collecting chamber and coiled into the surrounding area, apparently without ramifications (Fig. 45–47). These tubules were typical pusular elements, wrapped in what appeared to be a single large vesicle. The second set of pusular structures consisted of about 10 spherical to slightly elongated pusular vesicles, each with a constricted connection to the left-posterior side of the LFC (Fig. 42).

Molecular phylogeny. In the phylogenetic inference based on partial LSU rDNA sequences *S. cracoviense* formed a sister taxon to a large assemblage consisting of *Baldinia*, *Borghiella*,

Biecheleriopsis, *Biecheleria*, *Polarella*, *Protodinium*, and *Symbiodinium* (Fig. 49). Hence, *S. cracoviense* takes a basal position among dinoflagellates characterized by possessing eyespots of type B and type E sensu Moestrup and Daugbjerg (2007). This relationship was highly supported by a posterior probability of 1 and a bootstrap value of 87%. The lineage comprising *Sphaerodinium* and its close relatives formed an unresolved relationship with three distinct lineages, the orders Gonyaulacales and Dinophysales, and the family Tovelliaceae. This assemblage of diverse dinoflagellates was only moderately supported by a posterior probability of 0.78 and not supported by ML bootstrap analyses (<50%). Likewise our phylogenetic analyses of partial LSU rDNA sequences provided no reliable support for the deepest lineages.

DISCUSSION

Morphology and thecal structure. Although morphology and tabulation of the population of *Sphaerodinium* studied herein closely matches *S. cracoviense* as described by Wołoszyńska (1916), differences in the interpretation of particular plates result in different tabulation formulas. As shown here, the plate labelled Z is longitudinally aligned with the first apical plate and transversely links precingular plates on the left and right of the sulcus. It may be thought of as one of a complete ring of precingular plates, analogous to what is found in *Heterocapsa* F. Stein, *Fragilidium* A.R. Loeblich, and *Thecadinium* Kofoid & Skogsberg in the interpretations of Balech (1988, p. 160), Sournia (1986, p. 95), and Hoppenrath et al. (2005), respectively. In contrast, Wołoszyńska (1916) originally interpreted the plate as part of the sulcus, which she described as penetrating the epitheca. The depressed appearance of plate Z shown in an intact cell with a presumably incompletely developed theca in which cingular and sulcal margins are, for the most part, not raised, favours Wołoszyńska's interpretation. The analogous plate in several *Heterocapsa* species has also, contrary to Balech (1988), been labelled sulcal anterior (e.g. Hansen 1995; Iwataki 2008; Tamura, Iwataki, and Horiguchi 2005). However, when observed in well-developed thecae, plate Z was at the same level and had the same appearance as other epithecal plates, and was separated from the depressed sulcus by the raised upper margin of the cingulum.

Considering plate Z as part of the precingular ring, especially if it is labelled the first plate because of the alignment with the sulcus, forces the numbering of other precingular plates to change, resulting in an awkward position of plates compared with other thecate species. On the other hand, we prefer the interpretation that plates 1' and Z share the same orientation and are of similar width, and may be thought of as the result of the division of a single ancestral plate occupying a narrow strip from sulcus to apex.

The set of three small plates surrounded by the four apical plates of *Sphaerodinium* has hitherto been noted by terms equivalent to those used for the apical pore of peridinioids. However, as shown in our SEM, the apical pore of *S. cracoviense* appears quite distinct. The furrow with a row of knobs found in the narrow plate designated 1 brings to mind the apical furrow of some woloszynskioids, notably *Biecheleria* Moestrup, Lindberg & Daugbjerg and *Biecheleriopsis* Moestrup, Lindberg & Daugbjerg (Moestrup, Lindberg, and Daugbjerg 2009a, b). The general idea of the peridinioid apical complex includes a rectangular, somewhat elongate plate on the ventral side of a round pore plate that completely encircles a smaller platelet (Dodge and Hermes 1981; Toriumi and Dodge 1993). However, in *Tyrannodinium berolinense* (Lemmermann) Calado, Craveiro, Daugbjerg & Moestrup, and perhaps in some other pfisteriaceans (Litaker et al. 2005), the so-called plate X deeply notches the pore plate to the point of

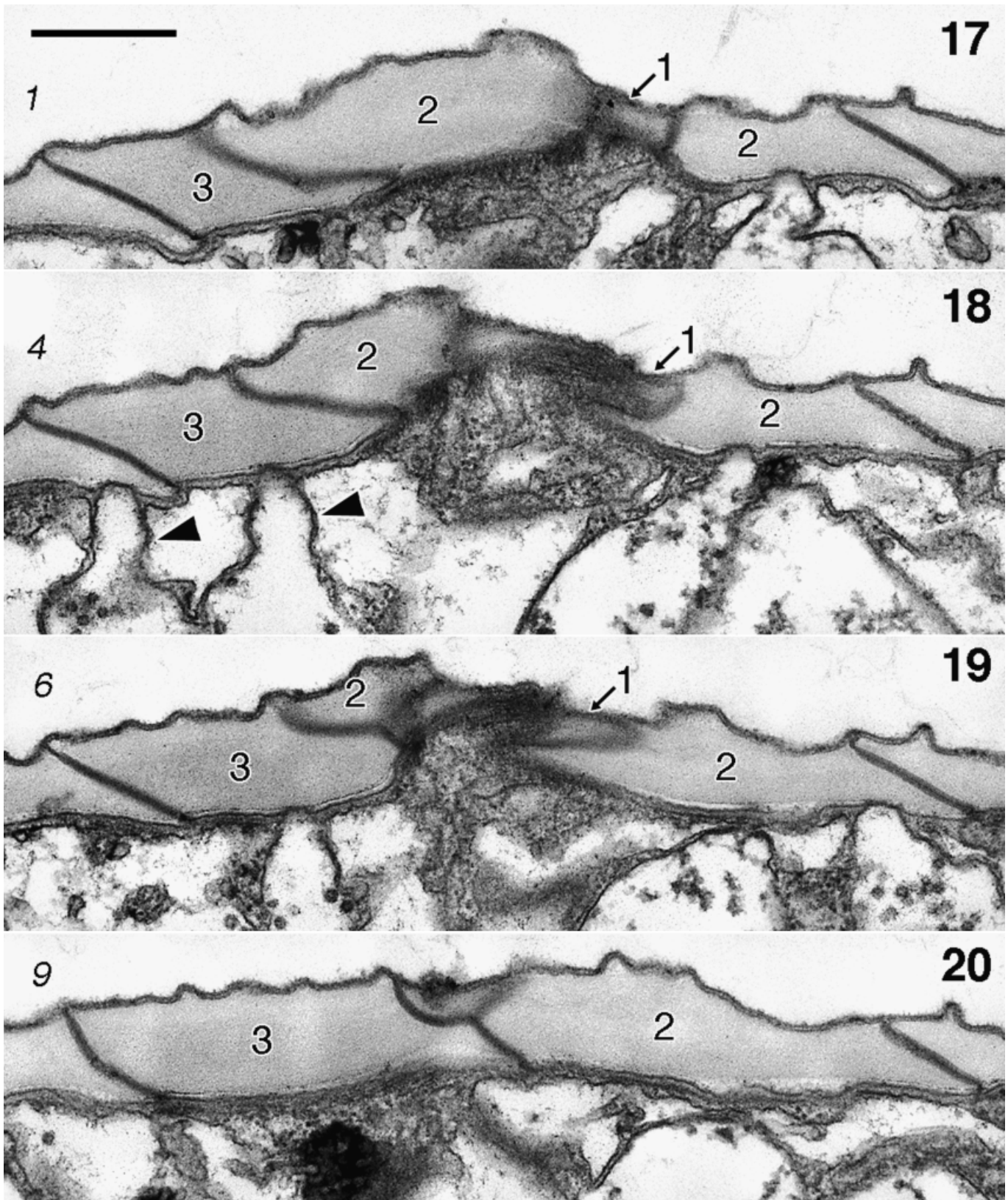


Fig. 17–20. *Sphaerodinium cracoviense*, transmission electron microscopy (TEM). Non-adjacent serial, longitudinal sections through the apical complex, proceeding approximately from left to right. Apical complex platelets are marked 1, 2, and 3, as in Fig. 13 and 14. Slanted numbers refer to the section number. Vesicles with tubular connections to amphiesmal vesicles are marked by arrowheads. Scale bar = 500 nm.

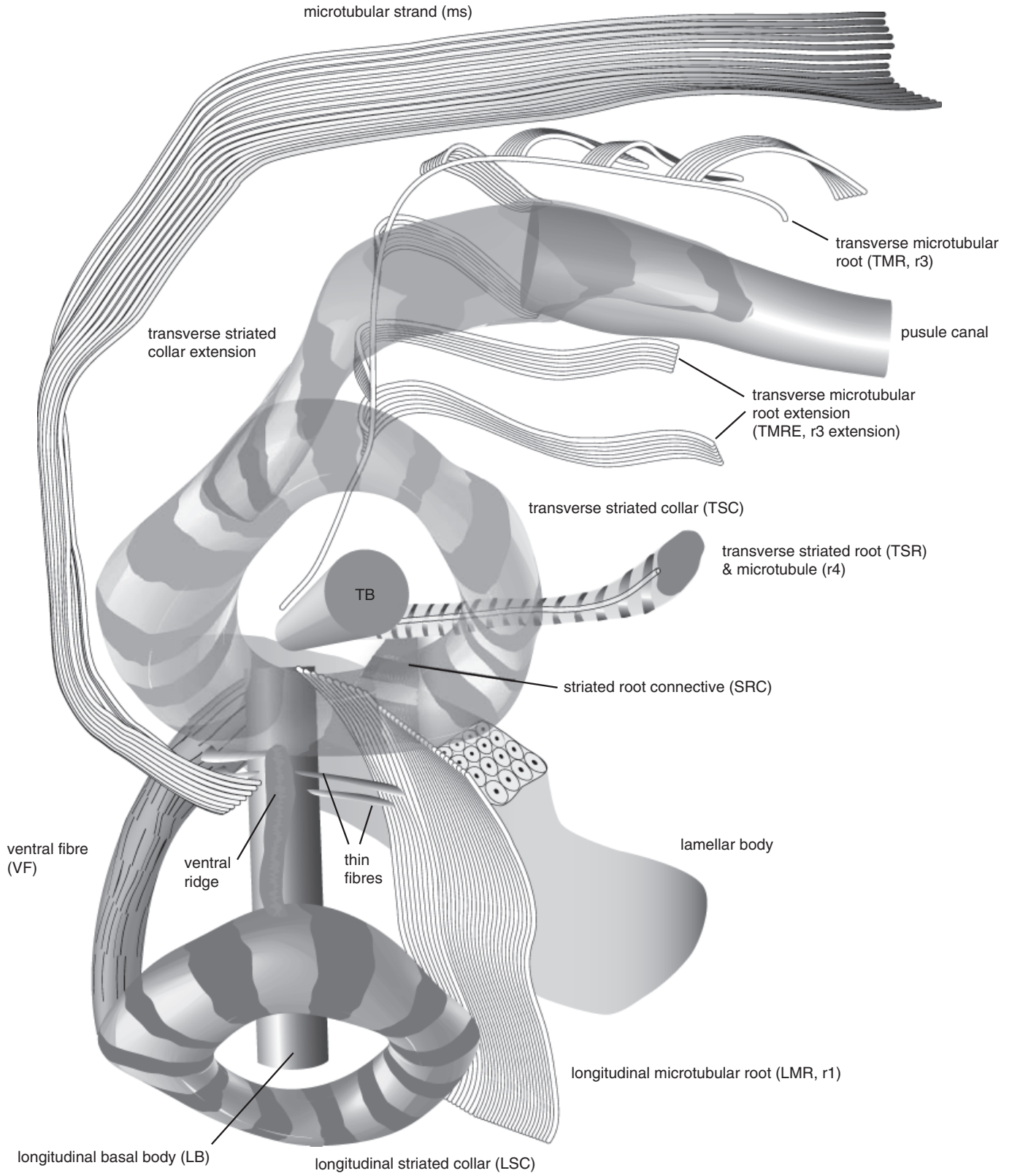


Fig. 21. Schematic reconstruction of the flagellar base area as seen from the left side of the cell. TB, transverse basal body. The transverse striated collar and its extension are rendered transparent to show underlying structures.

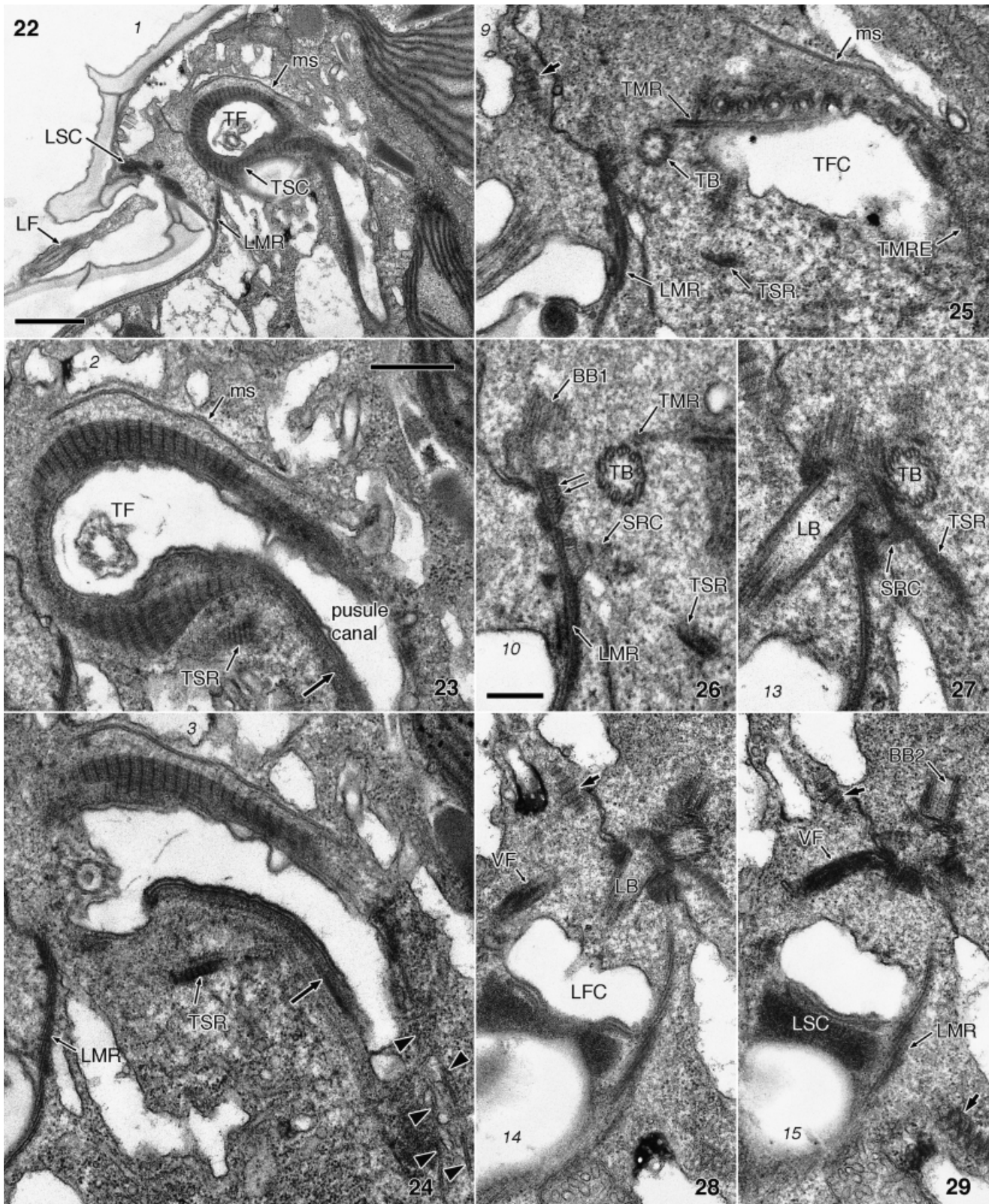


Fig. 22–29. *Sphaerodinium cracoviense*, transmission electron microscopy (TEM). Flagellar apparatus and microtubular strand (ms). Non-adjacent, nearly longitudinal serial sections proceeding from left to right. Slanted numbers refer to the section number. 22, 23. Transverse flagellum (TF) in the transverse flagellar canal (TFC). The transverse striated collar (TSC) is seen as a complete ring from which an extension branches off to the anterior side of the pusule canal. LF, longitudinal flagellum. Scale bar in Fig. 22 = 1 μ m. Scale bar in Fig. 23 = 500 nm. 24–27. The transverse microtubular root (TMR) and the transverse striated root (TSR) approach the transverse basal body (TB). Several rows of the transverse microtubular root extension (TMRE) are marked with arrowheads in Fig. 24. Note the dark material covering the terminal portion of the pusule canal (arrow in Fig. 24). SRC, striated root connective. The scale bar in Fig. 23 applies to Fig. 24 and 25. Scale in Fig. 26 = 200 nm; Fig. 26 and 27 to the same scale. 28, 29. The ventral fibre (VF) associates with the right side of the longitudinal basal body (LB). Short arrows indicate the lamellar body. LSC, longitudinal striated collar; BB1, BB2, replicated basal bodies. Same scale as Fig. 23.

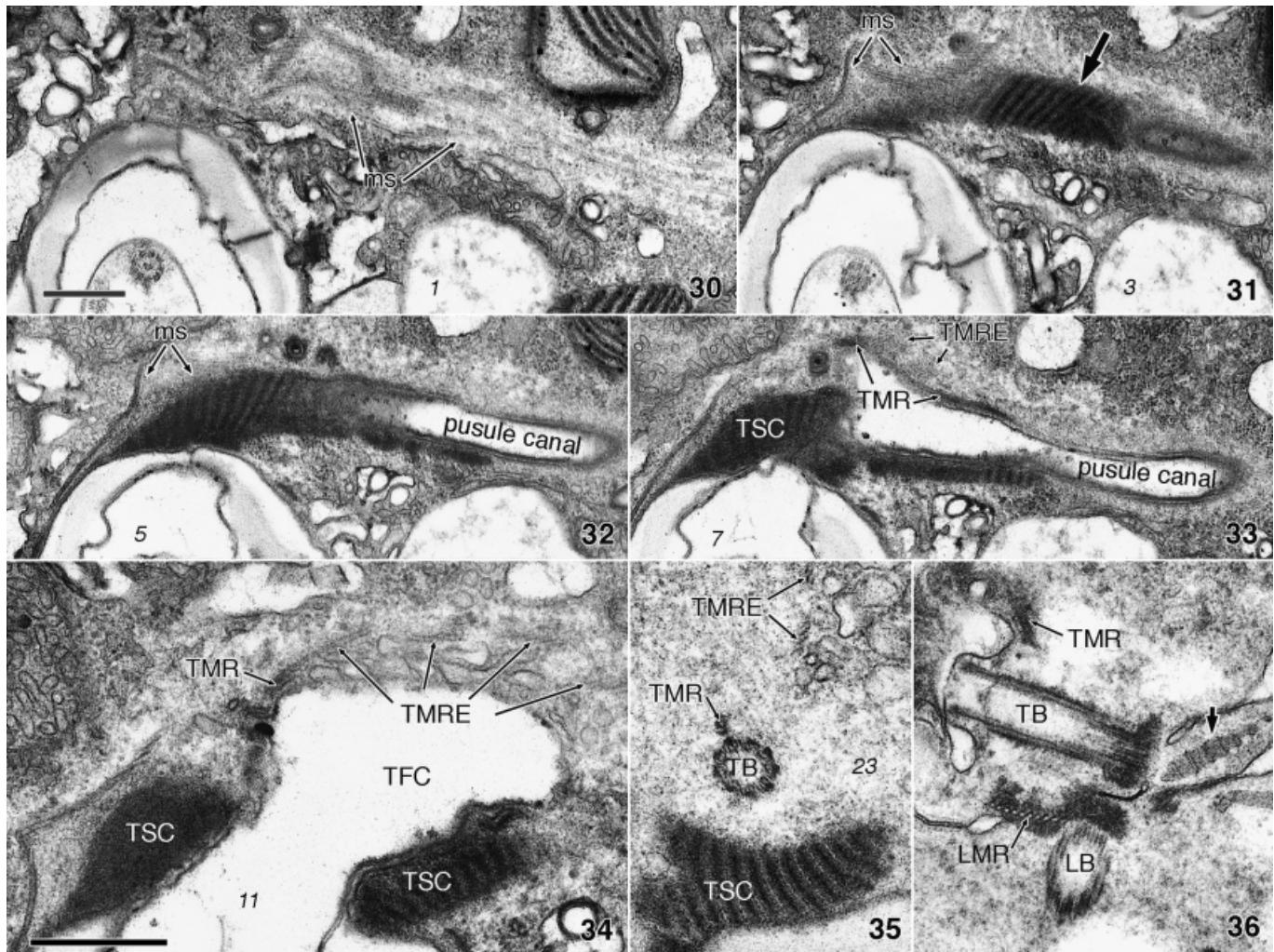


Fig. 30–36. *Sphaerodinium cracoviense*, transmission electron microscopy (TEM). Flagellar apparatus and microtubular strand (ms). Fig. 31–33, same scale as Fig. 30. Fig. 35–36, same scale as Fig. 34. Scale bars = 500 nm. 30–35. Non-adjacent, nearly longitudinal serial sections proceeding from left to right. Slanted numbers refer to the section number. 30–32. The ms follows a path roughly parallel to the extension (arrow) of the transverse striated collar (TSC) that runs along the pusule canal. 33–35. The transverse microtubular root (TMR) nucleates several groups of microtubules (TMRE) and ends adjacent to the anterior-proximal end of the transverse basal body (TB). 36. Anterior-dorsal view of the basal bodies of another cell, showing the proximal part of the longitudinal microtubular root (LMR). Note the lamellar body (short arrow). LB, longitudinal basal body.

appearing to form an incomplete ring (Calado et al. 2009). The possibility of a pore plate incompletely surrounding the small cover plate, which therefore touches plate X, suggests homology between *Sphaerodinium* plates 1, 2, and 3, and the cover plate, pore plate, and canal plate of peridinioids, respectively.

Flagellar base area. Although the overall organization of flagellar bases and roots of *S. cracoviense* is typical for dinoflagellates, several aspects are noteworthy. In addition to the three flagellar roots extending towards the cell's left, which occur in almost every dinoflagellate, some gonyaulacoids and all peridinioids examined in detail present a single-stranded root (SMR; r2 in Moestrup 2000) that associates obliquely with the right side of the LB (Calado and Moestrup 2002; Calado, Hansen, and Moestrup 1999; Calado et al. 2009; Craveiro et al. 2009a). This root seems to be absent in naked dinoflagellates, but has been reported in the woloszynskioid *Baldinia anauniensis* Gert Hansen & Daugbjerg (Hansen et al. 2007), which approaches *S. cracoviense* in several fine-structural and molecular aspects. The absence of an SMR in *S. cracoviense* is therefore surprising.

The occurrence of microtubules nucleated, either singly or in rows, along the TMR (r3) and extending towards the centre of the cell is a general dinoflagellate feature (e.g. Calado et al. 1999, 2006; Moestrup et al. 2009b). The orientation of the microtubular extensions of the TMR in *S. cracoviense* is remarkable in that they partially surround and follow the pusule canal near its attachment to the TFC, although whether they play any role in the orientation or functioning of the pusule is unknown.

The fibrous connection between TSR and LMR (SRC) is a common feature of dinoflagellate vegetative cells, except in the peridinioid group, where it is replaced by the so-called layered connective (LC), a possibly homologous structure which links, directly or indirectly, the basal bodies and the proximal ends of the two roots (Calado and Moestrup 2002; Calado et al. 1999; Craveiro et al. 2009a). An exception, insofar as *Heterocapsa* can be considered a true peridinioid, is the observation in *Heterocapsa pygmaea* A.R. Loeblich, R.J. Schmidt & Sherley of both an LC and an SRC (Bullman and Roberts 1986). The absence of an LC in *S. cracoviense* suggests a relatively distant relationship with the peridinioids.

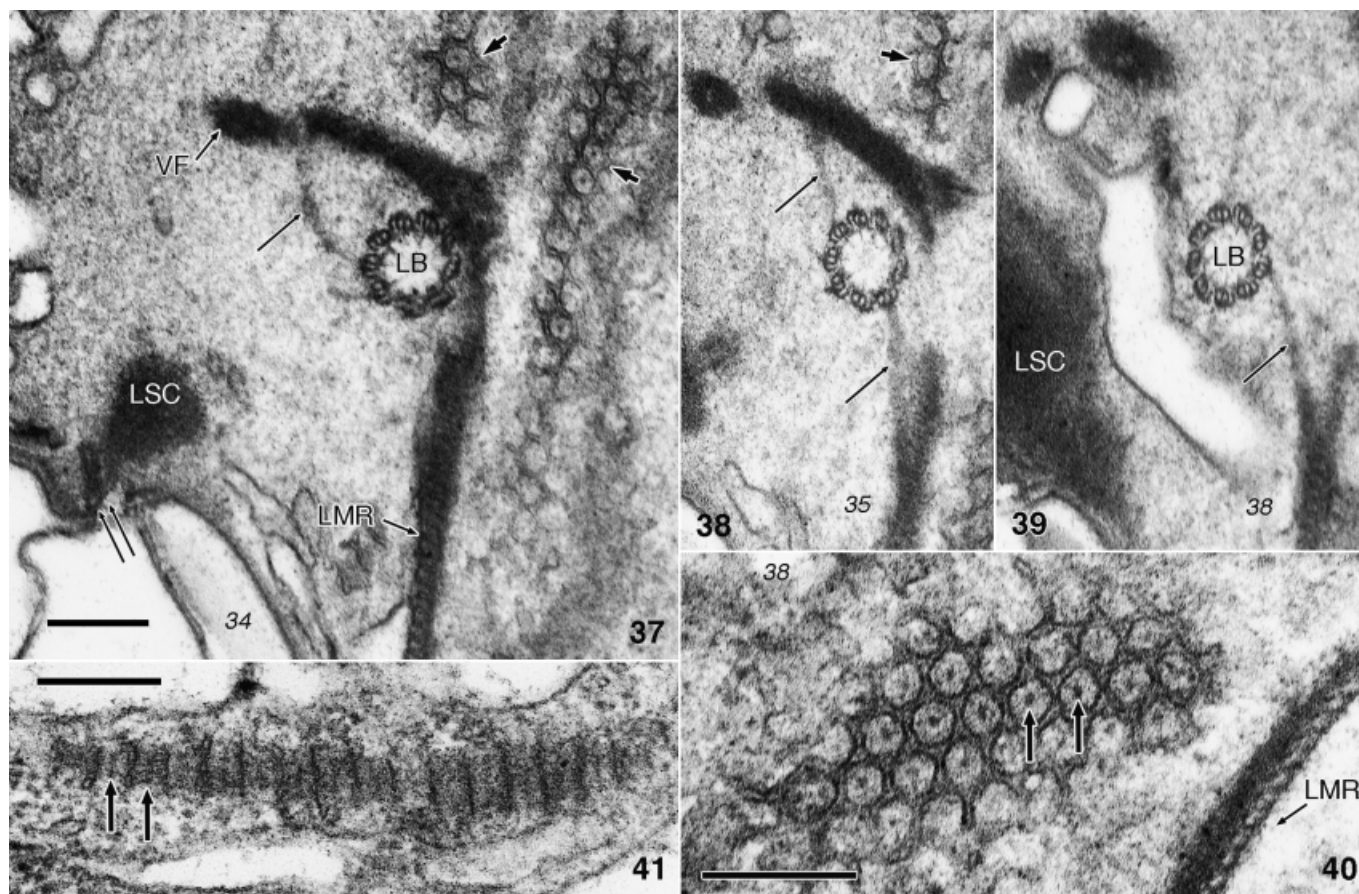


Fig. 37–41. *Sphaerodinium cracoviense*, transmission electron microscopy (TEM). Flagellar apparatus. Same series as in Fig. 30–35 except for Fig. 41. Fig. 37–39 have been tilted to provide a cross-sectional view of the longitudinal basal body (LB). Slanted numbers refer to the section number. 37–39. Apical view of the LB in cross section, showing the ventral fibre (VF) on the right side and the lamellar body (short arrows). Four connecting fibres are marked with thin arrows: two between the LB and the VF and two between the LB and the ventral side of the longitudinal microtubular root (LMR). LSC, longitudinal striated collar. 40, 41. Transverse and longitudinal sections (respectively) of the cell showing different aspects of the lamellar body. Arrows point to the electron-opaque central structure. Fig. 38–39, same scale as Fig. 37. Scale bars = 200 nm.

The prominent VF associated with the right side of the LB in *S. cracoviense* is remarkably similar to that described from *B. anauniensis*, not only in general aspect and orientation, but also in its connection to triplets of the LB through thin fibres (Hansen et al. 2007).

Fibrous connectives between triplets of the LB and the LMR, such as documented here for *S. cracoviense*, are common in athecate or thinly thecate dinoflagellates (e.g. *Esoptrodinium gemma* Javornický, *B. anauniensis*, *Symbiodinium natans* Gert Hansen & Daugbjerg; see Calado et al. 2006; Hansen and Daugbjerg 2009; Hansen et al. 2007), but not in peridinioids or gonyaulacoids.

Naked or thinly thecate dinoflagellates commonly have a variously prominent, oblique ridge in the area defined by the exit locations of the flagella and, if one is present, the peduncle (Calado, Craveiro, and Moestrup 1998; Dodge and Crawford 1968; Lindberg et al. 2005). Fine-structural analysis of these so-called ventral ridges shows a nearly longitudinal area lined by a single membrane and limited on both sides by fibrous material externally attached to amphiesmal vesicles. When a striated collar surrounding the exit point of a peduncle is present it is usually located near the anterior end of the ventral ridge (Calado et al. 1998, 2006). A relatively small ventral ridge was identified in *S. cracoviense* on the basis of its fine structure and the proximity

of its anterior end to the tip of a microtubular strand, here interpreted as homologous to those involved in peduncle extension. Its presence is noteworthy, as ventral ridges are not known to occur in peridinioids.

The membranous body showing a honeycomb pattern in transverse sections of the cell is strikingly similar to that found in *B. anauniensis* (Hansen et al. 2007). It brings to mind the stacked membranous structure found in the flagellar base area of *Kryptoperidinium foliaceum* (F. Stein) Er. Lindemann, a species containing a diatom-derived endosymbiont, and designated “lamellar body” (Dodge and Crawford 1969a, as *Glenodinium foliaceum* F. Stein). However, a honeycomb pattern is not visible in published material of *K. foliaceum* and was not found during recent re-examination of the lamellar body of this species from different angles (unpubl. data). Lamellar bodies were also reported from other species harbouring diatom-derived endosymbionts (e.g. *Peridinium quinquecornu* Abé, *Durinskia baltica* [K.M. Levander] Carty & El. R. Cox, and *Peridinium penardii* Lemmermann [Horiguchi and Pienaar 1991; Takano et al. 2008; Tomas and Cox 1973]). In addition to the lamellar body near the flagellar bases, sets of “orderly arranged stacked vesicles which appear as dilated smooth endoplasmic reticulum” were described adjacent to the peripherally located storage vacuoles of *D. baltica*; as shown in Fig. 42 in Tomas and Cox (1973) these structures resemble the

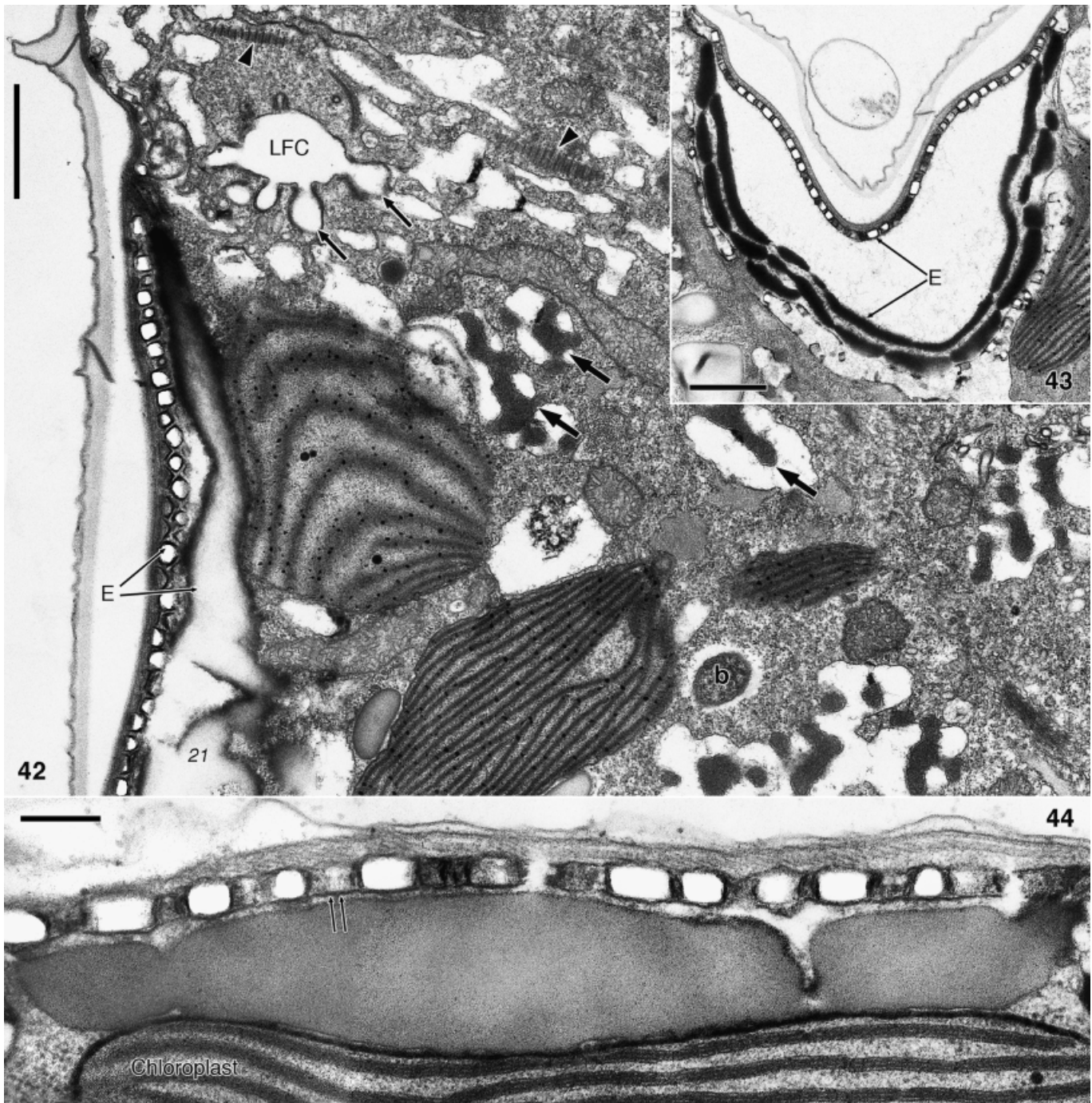


Fig. 42–44. *Sphaerodinium cracoviense*, transmission electron microscopy (TEM). Ventral region, eyespot, and pusular vesicles associated with the longitudinal flagellar canal (LFC). **42.** Longitudinal section, seen from the left side of the cell, through the ventral region showing the eyespot (E), and the LFC and attached pusular vesicles (thin arrows). Note the lamellar bodies (arrowheads). Electron-opaque microbodies (thick arrows) and associated vesicles are abundant in the ventral area. b, bacterium. Scale bar = 1 μm . **43.** Transverse section through both components of the eyespot. Scale bar = 1 μm . **44.** Higher magnification of the eyespot. Note the membrane of the vesicle evolving the brick-like components (double arrow) and the chloroplast lobe adjacent to the oil layer of the eyespot. Scale bar = 200 nm.

honeycomb pattern found in *S. cracoviense* and *B. anauniensis*. Although the strikingly similar lamellar bodies of *S. cracoviense* and *B. anauniensis* are plausibly homologous, as indicated by the general similarity of the flagellar apparatus and LSU-based phylogeny, there does not seem to be a close relationship between these two species and the diatom-bearing group. The possible role of the

lamellar body in phototaxis, mainly through analogy with the stacked membranes of light receptor cells of the retina, was discussed by Dodge and Crawford (1969a) and Hansen et al. (2007).

Microtubular strand, eyespot, and pusule. Microtubular strands located in the anterior-ventral area, near the basal bodies,

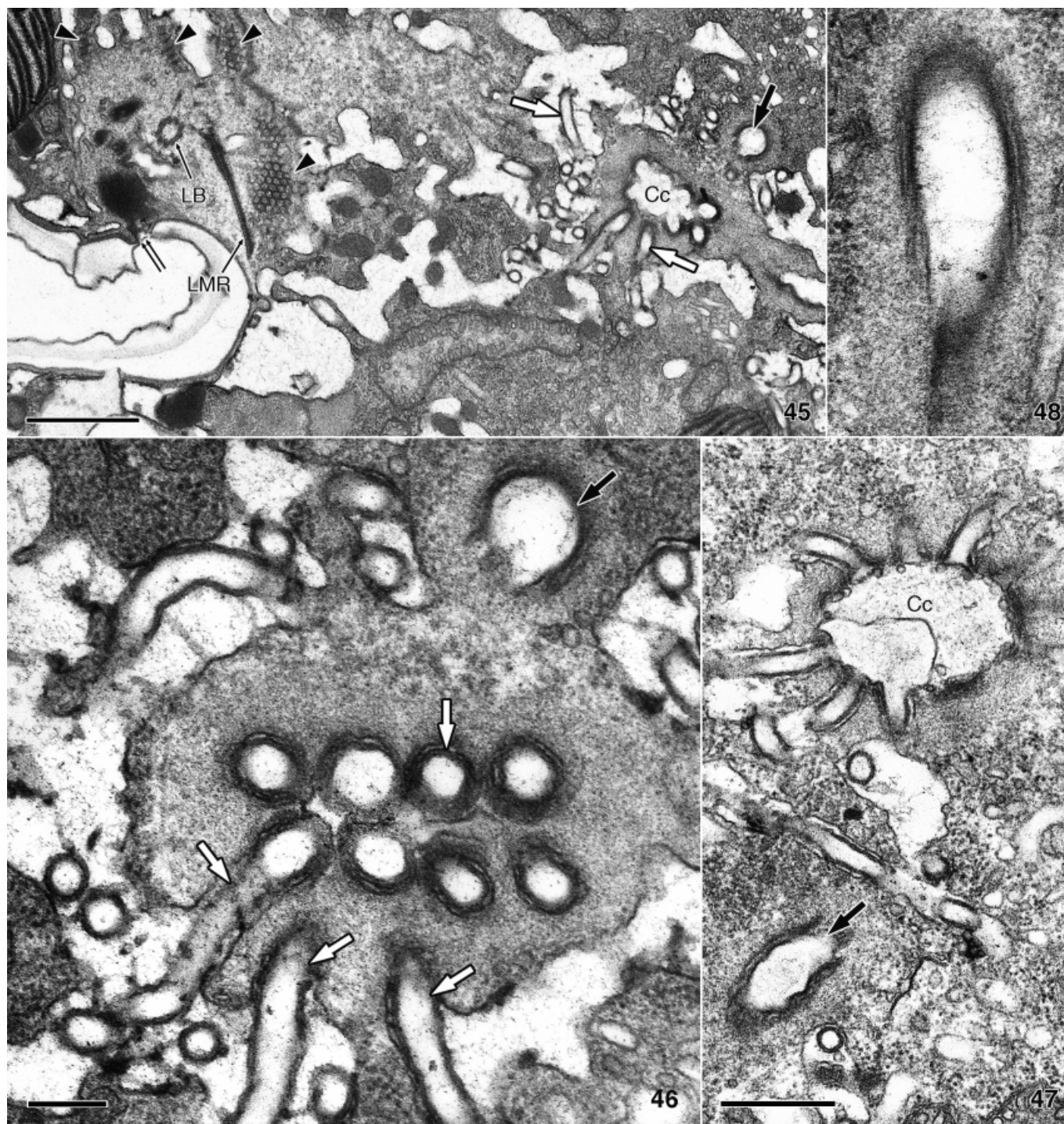


Fig. 45–48. *Sphaerodinium cracoviense*, transmission electron microscopy (TEM). Pusular system. 45–47. Localization of one of the pusular systems in relation to the basal body area. Some pusular tubules (white arrows) diverge from the collecting chamber (Cc, collecting chamber), which is an enlargement of the pusule canal (black arrow). Note the lamellar bodies (arrowheads) and the area of the ventral ridge (double arrow) in Fig. 45. LB, longitudinal basal body; LMR, longitudinal microtubular root. Scale bar = 1 μ m in Fig. 45. Scale bar = 200 nm in Fig. 46. Scale bar = 500 nm in Fig. 47. 48. Higher magnification of the pusule canal. Same scale as Fig. 46.

have been found in many dinoflagellates, both heterotrophic and autotrophic, examined in detail.

Cytoplasmic extensions from this ventral area, whatever their function, are typically supported by these microtubular strands,

and peduncles demonstrably involved in food uptake are associated with abundant electron-opaque vesicles (Calado et al. 1998, 2006; Hansen and Calado 1999). In *S. cracoviense*, as in *Palatinus apiculatus* Craveiro, Calado, Daugbjerg & Moestrup (Craveiro

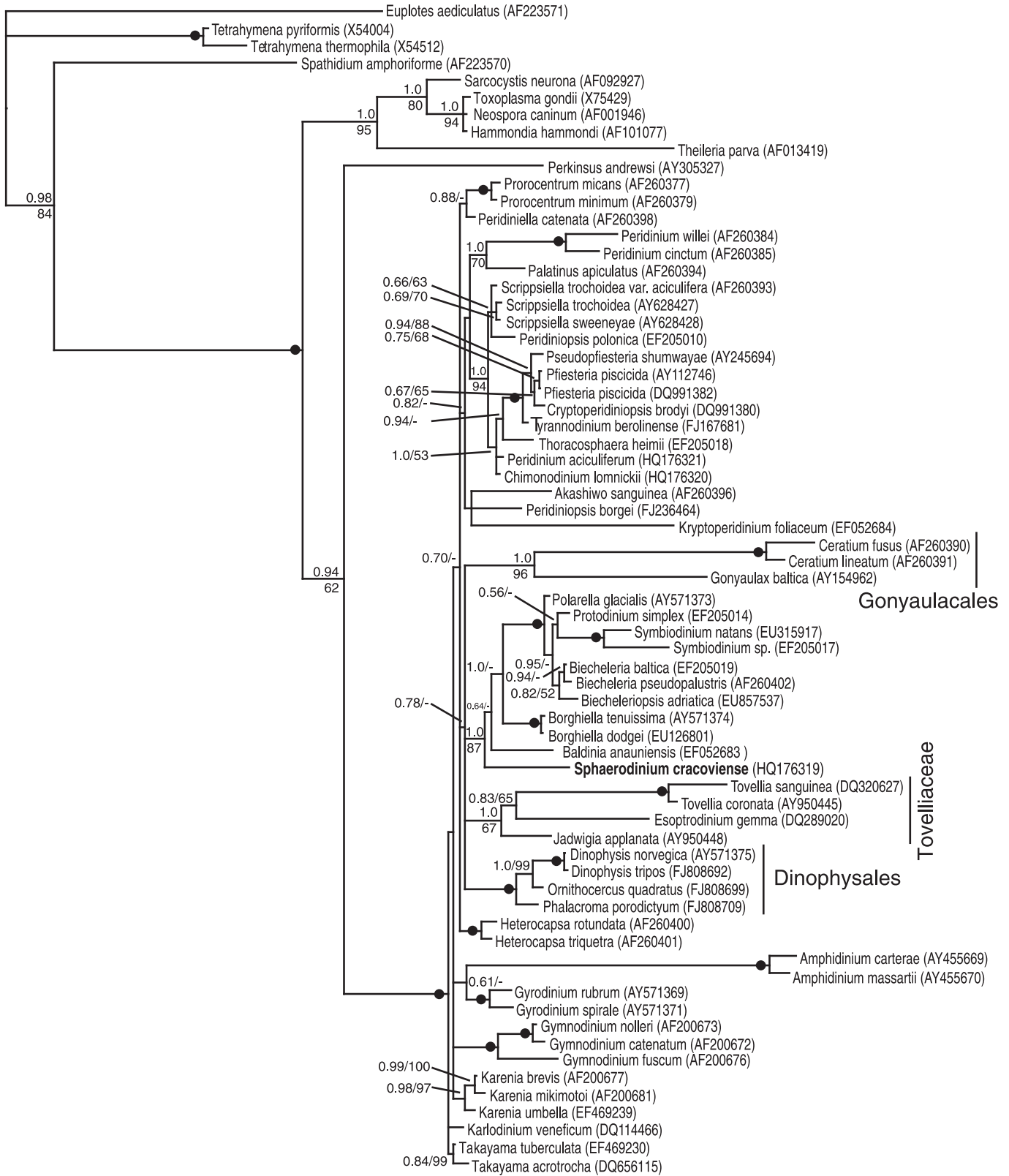


Fig. 49. Phylogeny of *Sphaerodinium cracoviense* and 57 other dinoflagellate species from Bayesian inference. The data matrix comprised 1,157 base pairs of nuclear-encoded large subunit rDNA and the dinoflagellate ingroup was polarized using ciliates, apicomplexans, and *Perkinsus*. Branch support values are written to the left of internodes. The first numbers are posterior probabilities from Bayesian inference (≥ 0.5) whereas the last numbers are from maximum likelihood bootstrap analyses with 500 replications ($\geq 50\%$). Maximum branch support (posterior probability = 1 and 100% in maximum likelihood bootstrap) is shown as filled black circles. Branch lengths are proportional to the number of character changes. *Sphaerodinium cracoviense* is boldfaced.

et al. 2009a), a microtubular strand not associated with opaque vesicles was found in the same location, and with the same orientation, as the ones extending into peduncles, but without reaching the cell surface and thereby suggesting that it is non-functional.

As recently reviewed (Moestrup and Daugbjerg 2007), and excluding the complex ocelloid of the Warnowiaceae (Greuet 1987), five different types of eyespot have been found previously in dinoflagellates: (1) type A, characterized by one to several layers of opaque globules inside a chloroplast lobe, as is commonly found in the eyespots of algae; (2) type B, in which a vesicle containing crystal-like units is located in the sulcal area, between the LMR (root 1) and an eyespot type A-like chloroplast lobe; (3) type C, made of opaque lipid globules not bounded by a membrane; (4) type D, in which layers of opaque globules are contained in a vesicle that is not connected to chloroplast lobes; and (5) type E, made of several layers of crystal-like units contained in a vesicle. The eyespot of *S. cracoviense* does not fit into any of these types. It is here proposed to represent a sixth, type F, characterized by a single layer of vesicle-contained crystal-like units overlying layers of more or less fused globules not bounded by membranes.

The pusular system of *S. cracoviense* is unusual. Most dinoflagellates have similar pusular types associated with each flagellar canal. In *Prosoaulax lacustris* (F. Stein) Calado & Moestrup a single pusular tube opens either at the transverse or at the longitudinal flagellar canal, leaving the other flagellar canal without associated pusule (Calado et al. 1998, as *Amphidinium lacustre* F. Stein, see Calado and Moestrup 2005). In all cells examined of *S. cracoviense*, different pusular types were associated with each flagellar canal. The pusular vesicles directly associated with part of the longitudinal flagellar canal resemble those of the pusules of *Amphidinium sensu stricto*, e.g. *Amphidinium rhynchocephalum* Anisimova (Farmer and Roberts 1989), and *Gymnodinium aureolum* (Hulburt) Gert Hansen (Hansen 2001). The pusule canal with an apparently fibrous cover that extends from the transverse flagellar canal of *S. cracoviense* is reminiscent of the one described from *Gymnodinium fuscum* (Ehrenberg) F. Stein (Dodge 1972; Dodge and Crawford 1969b). However, the inner dilated portion of the pusule canal of *G. fuscum* is associated with pusular vesicles instead of tubes. The pusule canal of *S. cracoviense* also bears some similarity with the tube extending from the longitudinal flagellar canal of *B. anauniensis*, which however, appeared lined in its distal part by amphiesmal vesicles and was interpreted as pusular in nature (i.e. with its internal membrane closely appressed to the inner membrane of an enveloping vesicle) (Hansen et al. 2007). Rows of pusular tubes opening to a collecting chamber have been described from *Karlodinium armiger* Bergholtz, Daugbjerg & Moestrup, although two similar pusules were present and the collecting chambers were directly associated with the flagellar canals (Bergholtz et al. 2005).

Phylogenetic affinities. Analysis of nuclear-encoded LSU rDNA provided high support for the position of *S. cracoviense* forming a sister taxon to woloszynskioid dinoflagellates possessing type B and type E eyespots. A substantial number of morphological features, as well as some missing structures, also seem to favour the somewhat isolated position of *S. cracoviense* between woloszynskioids with thin thecal plates (e.g. *Borghiella* and *Biecheleria*) and the peridinioids. In brief, these are the unique type F eyespot, the pusule system, the apical pore complex, and the number of postcingular plates, as well as features of the flagellar apparatus. The missing structures are the single-stranded root (r2) and the LC characteristic of peridinioids. Thus, the combination of genotypic and phenotypic characters may indicate that *Sphaerodinium* is distinct enough to warrant a new family or perhaps even a new order. However, we refrain from proposing a new

family for *Sphaerodinium* until additional species of the genus have been examined in detail by electron microscopy and at the molecular level, and the number of comparison points from within the neighbouring groups has increased.

The molecular data also suggest an affinity between *Sphaerodinium* and *Baldinia*. This is reflected in some very detailed morphological features like the VF being associated with the right side of the longitudinal basal body and the honeycomb pattern in transverse sections in both species. However, there are also a number of conspicuous differences separating *Sphaerodinium* and *Baldinia* at family level, notably the structure of the eyespot and the fact that *Baldinia* is an unarmoured species.

In conclusion, the arrangement of thecal plates of *S. cracoviense*, which fits the concept of peridinioids as defined, for example, by Taylor (2004), is contradicted by genotypic and phenotypic features that strongly indicate a closer relationship to several woloszynskioid groups than to *Peridinium* and its splinter genera, and the Pfiesteriaceae.

ACKNOWLEDGMENTS

Thanks to Prof. Konrad Wołowski and Dr. Elżbieta Wilk-Woźniak for assistance and hospitality when visiting and collecting near Cracow, Poland, in August 2007. Karin Lindberg participated in the field work and helped with the SEM. SCC was supported by a grant from the financing programme POCL, Portugal (SFRH/BD/16794/2004) and a grant from the European Commission's (FP 6) Integrated Infrastructure Initiative programme SYNTHESYS (DK-TAF) during July–September 2008. ND thanks the Carlsbergfondet for equipment grants.

LITERATURE CITED

- Balech, E. 1988. Los dinoflagelados del Atlantico Sudoccidental. *Publ. Espec. Inst. Esp. Oceanogr.*, 1:1–310.
- Bergholtz, T., Daugbjerg, N., Moestrup, Ø. & Fernández-Tejedor, M. 2005. On the identity of *Karlodinium veneficum* and description of *Karlodinium armiger* sp. nov. (Dinophyceae), based on light and electron microscopy, nuclear-encoded LSU rDNA, and pigment composition. *J. Phycol.*, 42:170–193.
- Bullman, V. & Roberts, K. R. 1986. Structure of the flagellar apparatus in *Heterocapsa pygmaea* (Pyrrophyta). *Phycologia*, 25:558–571.
- Calado, A. J. & Moestrup, Ø. 2002. Ultrastructural study of the type species of *Peridiniopsis*, *Peridiniopsis borgei* (Dinophyceae), with special reference to the peduncle and flagellar apparatus. *Phycologia*, 41:567–584.
- Calado, A. J. & Moestrup, Ø. 2005. On the freshwater dinoflagellates presently included in the genus *Amphidinium*, with a description of *Prosoaulax* gen. nov. *Phycologia*, 44:112–119.
- Calado, A. J., Craveiro, S. C. & Moestrup, Ø. 1998. Taxonomy and ultrastructure of a freshwater, heterotrophic *Amphidinium* (Dinophyceae) that feeds on unicellular protists. *J. Phycol.*, 34:536–554.
- Calado, A. J., Hansen, G. & Moestrup, Ø. 1999. Architecture of the flagellar apparatus and related structures in the type species of *Peridinium*, *P. cinctum* (Dinophyceae). *Eur. J. Phycol.*, 34:179–191.
- Calado, A. J., Craveiro, S. C., Daugbjerg, N. & Moestrup, Ø. 2006. Ultrastructure and LSU rDNA-based phylogeny of *Esotrodinium gemma* (Dinophyceae), with notes on feeding behavior and the description of the flagellar base area of a planozygote. *J. Phycol.*, 42:434–452.
- Calado, A. J., Craveiro, S. C., Daugbjerg, N. & Moestrup, Ø. 2009. Description of *Tyrannodinium* gen. nov., a freshwater dinoflagellate closely related to the marine *Pfiesteria*-like species. *J. Phycol.*, 45:1195–1205.
- Caljon, A. G. 1987. Phytoplankton of a recently landlocked brackish-water lagoon of Lake Tanganyika: a systematic account. *Hydrobiologia*, 153:31–54.
- Carty, S. & Wujek, D. E. 2003. A new species of *Peridinium* and new records of dinoflagellates and silica-scaled chrysophytes from Belize. *Caribb. J. Sci.*, 39:136–139.

- Christensen, T. 1962. Alger i naturen og i laboratoriet. 1st ed. Nucleus, Copenhagen, Denmark, p. 1–136 (in Danish).
- Couté, A. & Iltis, A. 1984. Mise au point sur la flore péridiniale (Algae, Pyrrophyta) d'eau douce de Côte d'Ivoire. *Rev. Hydrobiol. Trop.*, **17**:53–64.
- Craveiro, S. C., Calado, A. J., Daugbjerg, N. & Moestrup, Ø. 2009a. Ultrastructure and LSU rDNA-based revision of *Peridinium* group palatinum (Dinophyceae) with the description of *Palatinus* gen. nov. *J. Phycol.*, **45**:1175–1194.
- Craveiro, S. C., Calado, A. J., Daugbjerg, N. & Moestrup, Ø. 2009b. Fine structure and phylogeny of *Sphaerodinium*, an unusual freshwater dinoflagellate. Abstract. *Phycologia*, **48**:23–24.
- Daugbjerg, N., Hansen, G., Larsen, J. & Moestrup, Ø. 2000. Phylogeny of some of the major genera of dinoflagellates based on ultrastructure and partial LSU rDNA sequence data, including the erection of three new genera of unarmoured dinoflagellates. *Phycologia*, **39**:302–317.
- Dodge, J. D. 1972. The ultrastructure of the dinoflagellate pusule: a unique osmo-regulatory organelle. *Protoplasma*, **75**:285–302.
- Dodge, J. D. & Crawford, R. M. 1968. Fine structure of the dinoflagellate *Amphidinium carteri* Hulbert. *Protistologica*, **4**:231–242, +pls 1–6.
- Dodge, J. D. & Crawford, R. M. 1969a. Observations on the fine structure of the eyespot and associated organelles in the dinoflagellate *Glenodinium foliaceum*. *J. Cell Sci.*, **5**:479–493.
- Dodge, J. D. & Crawford, R. M. 1969b. The fine structure of *Gymnodinium fuscum*. *New Phytol.*, **68**:613–618.
- Dodge, J. D. & Hermes, H. B. 1981. A scanning electron microscopical study of the apical pores of marine dinoflagellates (Dinophyceae). *Phycologia*, **20**:424–430.
- Farmer, M. A. & Roberts, K. R. 1989. Comparative analyses of the dinoflagellate flagellar apparatus. III. Freeze substitution of *Amphidinium rhynchocephalum*. *J. Phycol.*, **25**:280–292.
- Felsenstein, J. 2008. Phylogeny Inference Package (PHYLIP). Version 3.68. University of Washington, Seattle.
- Greuet, C. 1987. Complex organelles. In: Taylor, F. J. R. (ed.), *The Biology of Dinoflagellates*. Blackwell Scientific Publications, Oxford, p. 117–142.
- Grigorszky, I., Borics, G., Padišák, J., Tótmérész, B., Vasas, G., Nagy, S. & Borbély, G. 2003. Factors controlling the occurrence of *Dinophyta* species in Hungary. *Hydrobiologia*, **506–509**:203–207.
- Guindon, S. & Gascuel, O. 2003. A simple, fast, and accurate algorithm to estimate large phylogenies by maximum likelihood. *Syst. Biol.*, **52**:696–704.
- Hansen, G. 1995. Analysis of the thecal plate pattern in the dinoflagellate *Heterocapsa rotundata* (Lohmann) comb. nov. (= *Katodinium rotundatum* (Lohmann) Loeblich). *Phycologia*, **34**:166–170.
- Hansen, G. 2001. Ultrastructure of *Gymnodinium aureolum* (Dinophyceae): toward a further redefinition of *Gymnodinium sensu stricto*. *J. Phycol.*, **37**:612–623.
- Hansen, G. & Daugbjerg, N. 2004. Ultrastructure of *Gyrodinium spirale*, the type species of *Gyrodinium* (Dinophyceae), including a phylogeny of *G. dominans*, *G. rubrum* and *G. spirale* deduced from partial LSU rDNA sequences. *Protist*, **155**:271–294.
- Hansen, G. & Daugbjerg, N. 2009. *Symbiodinium natans* sp. nov.: a “free-living” dinoflagellate from Tenerife (Northeast-Atlantic Ocean). *J. Phycol.*, **45**:251–263.
- Hansen, G., Daugbjerg, N. & Henriksen, P. 2000. Comparative study of *Gymnodinium mikimotoi* and *Gymnodinium aureolum*, comb. nov. (= *Gyrodinium aureolum*) based on morphology, pigment composition, and molecular data. *J. Phycol.*, **36**:394–410.
- Hansen, G., Daugbjerg, N. & Henriksen, P. 2007. *Baldinia anauniensis* gen. et sp. nov.: a “new” dinoflagellate from Lake Tovel, N. Italy. *Phycologia*, **46**:86–108.
- Hansen, P. J. & Calado, A. C. 1999. Phagotrophic mechanisms and prey selection in free-living dinoflagellates. *J. Eukaryot. Microbiol.*, **46**:382–389.
- Hoppenrath, M., Bolch, C. J. S., Yoshimatsu, S., Saldarriaga, J. F., Schweikert, M., Campbell, C. N., Toriumi, S., Dodge, J. D., Elbrächter, M. & Taylor, F. J. R. 2005. Nomenclatural note on a *Thecadinium* species (Dinophyceae, Gonyaulacales), which was described as new independently three times within two months. *J. Phycol.*, **41**:1284–1286.
- Horiguchi, T. & Pienaar, R. N. 1991. Ultrastructure of a marine dinoflagellate, *Peridinium quinquecorne* Abé (Peridinales) from South Africa with particular reference to its chrysophyte endosymbiont. *Bot. Mar.*, **34**:123–131.
- Iwataki, M. 2008. Taxonomy and identification of the armored dinoflagellate genus *Heterocapsa* (Peridinales, Dinophyceae). *Plankton Benthos Res.*, **3**:135–142.
- Lenaers, G., Maroteaux, L., Michot, B. & Herzog, M. 1989. Dinoflagellate in evolution. A molecular phylogenetic analysis of large subunit ribosomal RNA. *J. Mol. Evol.*, **29**:40–51.
- Lindberg, K., Moestrup, Ø. & Daugbjerg, N. 2005. Studies on woloszynskioid dinoflagellates I: *Woloszynskia coronata* re-examined using light and electron microscopy and partial LSU rDNA sequences, with description of *Tovellia* gen. nov. and *Jadwigia* gen. nov. (Tovelliaceae fam. nov.). *Phycologia*, **44**:416–440.
- Ling, H. U., Croome, R. L. & Tyler, P. A. 1989. Freshwater dinoflagellates of Tasmania, a survey of taxonomy and distribution. *Br. Phycol. J.*, **24**:111–129.
- Litaker, R. W., Steidinger, K. A., Mason, P. L., Landsberg, J. H., Shields, J. D., Reece, K. S., Haas, L. W., Vogelbein, W. K., Vandersea, M. W., Kibler, S. R. & Tester, P. A. 2005. The reclassification of *Pfiesteria shumwayae*: *Pseudopfiesteria*, gen. nov. *J. Phycol.*, **41**:643–651.
- Loeblich, A. R. Jr. & Loeblich, A. R. III 1966. Index to the genera, subgenera, and sections of the Pyrrophyta. *Stud. Trop. Oceanogr.*, **3**:i–ix, 1–94.
- Moestrup, Ø. 2000. The flagellate cytoskeleton. Introduction of a general terminology for microtubular flagellar roots in protists. In: Leadbeater, B. S. C. & Green, J. C. (ed.), *The Flagellates. Unity, Diversity and Evolution*. Systematics Association Special Volume No. 59. Taylor & Francis, New York, p. 69–94.
- Moestrup, Ø. & Daugbjerg, N. 2007. On dinoflagellate phylogeny and classification. In: Brodie, J. & Lewis, J. (ed.), *Unravelling the Algae, the Past, Present, and Future of Algal Systematics*. Systematics Association Special Volume No. 75. CRC Press, Boca Raton, p. 215–230.
- Moestrup, Ø., Lindberg, K. & Daugbjerg, N. 2009a. Studies on woloszynskioid dinoflagellates IV. The genus *Biecheleria* gen. nov. *Phycol. Res.*, **57**:203–220.
- Moestrup, Ø., Lindberg, K. & Daugbjerg, N. 2009b. Studies on woloszynskioid dinoflagellates V. Ultrastructure of *Biecheleriopsis* gen. nov., with description of *Biecheleriopsis adriatica* sp. nov. *Phycol. Res.*, **57**:221–237.
- Posada, D. & Crandall, K. A. 1998. MODELTEST: testing the model of DNA substitution. *Bioinformatics*, **14**:817–818.
- Ronquist, F. & Huelsenbeck, J. P. 2003. MRBAYES 3: Bayesian phylogenetic inference under mixed models. *Bioinformatics*, **19**:1572–1574.
- Schiller, J. 1935. Dinoflagellatae (Peridineae) in monographischer Behandlung. In: Kolkwitz, R. (ed.), *Rabenhorst's Kryptogamenflora von Deutschland, Österreichs und der Schweiz*, 2nd ed., vol. 10 (3). Part 2, Issue 1. Akademische Verlagsgesellschaft, Leipzig, Germany, p. 1–160.
- Sournia, A. 1986. Atlas du Phytoplancton Marin. Vol. 1. Introduction, Cyanophycées, Dictyochophycées, Dinophycées et Raphidophycées. Éditions du Centre National de la Recherche Scientifique, Paris, 219 p.
- Swofford, D. L. 2003. PAUP* Phylogenetic Analysis Using Parsimony (*and Other Methods), Version 4. Sinauer Associates, Sunderland, MA, USA.
- Takano, Y., Hansen, G., Fujita, D. & Horiguchi, T. 2008. Serial replacement of diatom endosymbionts in two freshwater dinoflagellates, *Peridiniopsis* spp. (Peridinales, Dinophyceae). *Phycologia*, **47**:41–53.
- Tamura, M., Iwataki, M. & Horiguchi, T. 2005. *Heterocapsa psammophila* sp. nov. (Peridinales, Dinophyceae), a new sand-dwelling marine dinoflagellate. *Phycol. Res.*, **53**:303–311.
- Taylor, F. J. R. 2004. Illumination or confusion? Dinoflagellate molecular phylogenetic data viewed from a primarily morphological standpoint. *Phycol. Res.*, **52**:308–324.
- Thompson, R. H. 1951. A new genus and new records of freshwater Pyrrophyta in the Desmokyntae and Dinophyceae. *Lloydia*, **13**:277–299.

- Tolotti, M. & Thies, H. 2002. Phytoplankton community and limnochemistry of Piburger See (Tyrol, Austria) 28 years after lake restoration. *J. Limnol.*, **61**:77–88.
- Tomas, R. N. & Cox, E. R. 1973. Observations on the symbiosis of *Peridinium balticum* and its intracellular alga. I. Ultrastructure. *J. Phycol.*, **9**:304–323.
- Toriumi, S. & Dodge, J. D. 1993. Thecal apex structure in the Peridiniaceae (Dinophyceae). *Eur. J. Phycol.*, **28**:39–45.
- Wołoszyńska, J. 1916. Polnische Süßwasser-Peridineen. *Bull. Int. Acad. Sci. Cracovie, Cl. Sci. Math., Sér. B: Sci. Nat.*, **1915**:260–285, pl. 10–14.
- Wołoszyńska, J. 1930. Beitrag zur Kenntnis des Phytoplanktons tropischer Seen. *Arch. Hydrobiol. i Ryb.*, **5**:159–169.

Received: 07/08/10, 08/24/10; accepted: 08/26/10